Supporting Information for

"Electrically Controlled Adsorption of Oxygen in Bilayer Graphene Devices"

Yoshiaki Sato, Kazuyuki Takai, and Toshiaki Enoki *

Department of Chemistry, Tokyo Institute of Technology, 2-12-1 Ookayama, Meguro-ku, Tokyo, 152-8551, Japan

1 Experimental method

Graphene flakes were mechanically exfoliated from highly oriented pyrolytic graphite (HOPG) and transferred onto 300 nm thick SiO_2 on heavily n^{++}-doped Si substrate (less than 0.02 Ω cm). The number of layers was identified with optical microscopy and micro Raman spectroscopy, and we selected BLG with the Bernal stacking.[1–4] The D-band signal ($\approx$ 1350 cm^{-1}) was hardly observed, which confirmed that graphene flakes used in this study was less defective. We used photolithography rather than e-beam lithography for electrodes patterning to avoid imprinting lattice defects caused by e-beam irradiation.[5] We used OAP (Tokyo Ohka Co.) and TSMR-8900LB (Tokyo Ohka Co.) as photoresist. Depositing Au/Cr (45 nm / 5 nm) followed by lift-off, we acquired back-gate-type FET devices with two-probe geometries. The conductivity was measured in a small-scale vacuum chamber the basal pressure of which is under 10^{-4} Pa. The volume of the vacuum chamber is designed to be small enough compared to the flow rate of the turbo molecular pump system, so that 1 atm of gaseous oxygen can be evacuated in several seconds below the pressure of 10^{-1} Pa. The drain-source current was set to 0.3–0.5 μA.

* Corresponding author. E-mail: enoki.t.aa@m.chem.titech.ac.jp, FAX: +81-3-5734-2242

2 Electrochemical description in the charge transfer

The net electric current from the electrode to the redox molecules is obtained as a consequence of compensation between the anodic partial current density j_{OX} (the electron transfer from the reduced molecules to the electrode) and the cathodic partial current density j_{RED} (the electron transfer from the electrode to the oxidized molecules), that is,

$$J = (j_{\mathrm{OX}} - j_{\mathrm{RED}})A_{\mathrm{elec}}, \tag{S1}$$

where A_{elec} is the surface area of the electrode. According to Butler–Volmer equation,[6] each partial current is given by

$$j_{\mathrm{OX}} = j_0(T)\exp\left(\frac{(1-\beta)Z_{\mathrm{CT}}}{k_{\mathrm{B}}T}e\eta\right), \tag{S2a}$$

$$j_{\mathrm{RED}} = j_0(T)\exp\left(-\frac{\beta Z_{\mathrm{CT}}}{k_{\mathrm{B}}T}e\eta\right), \tag{S2b}$$

where β is the symmetry factor[6], Z_{CT} is the number of the electrons involved in the redox reaction, and η is the overpotential defined by $\eta := E - E_{\mathrm{eq}}$ (E is the electric potential of the electrode and E_{eq} is the electric potential in equilibrium). When the system is in the equilibrium, i.e., $\eta = 0$, $j_{\mathrm{OX}} = j_{\mathrm{RED}} = j_0(T)$ is fulfilled, and the net current is equal to zero. Note that $j_0(T)$ represents the (gross) rate for charge transfer, and depends on temperature as $j_0(T) \propto \exp\left(-{}^{\ddagger}E_{\mathrm{eq}}/k_{\mathrm{B}}T\right)$ (${}^{\ddagger}E_{\mathrm{eq}}$ is the energy barrier of the electron tunneling when $j_{\mathrm{OX}} = j_{\mathrm{RED}}$, namely, in the equilibrium condition). When $\eta < 0$, the electron transfer from the electrode to the molecules prevails and when $\eta > 0$, the electron transfer occurs in the opposite direction.

Our electrochemical description of the charge transfer between graphene and the adsorbing molecules assumes that graphene serves as the electrode. In the case shown in Figure 5 in the main part, the overpotential corresponds to $-e\eta = -\Delta G = \zeta_{\mathrm{G}} - \zeta_{\mathrm{ads}} > 0$. If $\zeta_{\mathrm{G}} - \zeta_{\mathrm{ads}} \gg k_{\mathrm{B}}T$ is fulfilled, we can envisage $J \simeq -j_{\mathrm{RED}}A_{\mathrm{elec}}$. Then the frequency of the charge transfer is given by

$$\begin{aligned}\frac{\mathrm{d}N_{\mathrm{ox}}}{\mathrm{d}t} = \frac{-J}{eA_{\mathrm{elec}}} &\propto \exp\left(-\frac{{}^{\ddagger}E_{\mathrm{eq}}}{k_{\mathrm{B}}T}\right)\exp\left(-\frac{\beta Z_{\mathrm{CT}}}{k_{\mathrm{B}}T}e\eta\right) \\ &= \exp\left(\frac{-{}^{\ddagger}E_{\mathrm{eq}} + \beta Z_{\mathrm{CT}}\{\varepsilon_{\mathrm{F}} + (\zeta_{\mathrm{CNP}} - \zeta_{\mathrm{ads}})\}}{k_{\mathrm{B}}T}\right),\end{aligned} \tag{S3}$$

where $\varepsilon_F = \zeta_G - \zeta_{CNP}$. We note that Eq. (S3) is equivalent to the Arrhenius equation with the activation energy ${}^{\ddagger}E = {}^{\ddagger}E_{eq} + \beta Z_{CT} e\eta = {}^{\ddagger}E_{eq} - \beta Z_{CT}\{\varepsilon_F + (\zeta_{CNP} - \zeta_{ads})\}$. In the simple redox reaction as above, the transfer coefficient is given by $\alpha' = Z_{CT}\beta$ (i.e., $\mathrm{d}^{\ddagger}E = \alpha' e\eta$).[6] Then we have the expression for the change of the activation energy upon the Fermi energy and the equilibrium potential as

$$\mathrm{d}^{\ddagger}E = -\alpha' \mathrm{d}\varepsilon_F - \alpha' \mathrm{d}(\zeta_{CNP} - \zeta_{ads}) + \delta^{\ddagger}E, \tag{S4}$$

where we add the term $\delta^{\ddagger}E$ to take into account the other effects that do not change the Fermi level nor the equilibrium potential, but change the activation energy. Molecular adsorption with charge transfer should change both of ε_F and $\zeta_{CNP} - \zeta_{ads}$, which leads to change in ${}^{\ddagger}E$ according to Eq. (S4). We can classify the possible adsorption effects into four categories:

Type I: *The change of ε_F through the charge doping to graphene.* When carrier injection or rejection occurs to graphene by molecular adsorption or the application of the gate electric field, the Fermi level changes so that ${}^{\ddagger}E$ changes. Since zero-gap semiconductor graphene (or even bilayer graphene) has low density of states near the Fermi level, the small amount of charge induced to graphene brings large (> 0.1 eV) shift. Thus Type I effect governs the change in ${}^{\ddagger}E$ accompanied with the molecular adsorption.

Type II-a: *The change in ζ_{ads} associated with the increase of the adsorbed molecules.* According to the Nernst equation, the equilibrium potential depends on the concentration of the adsorbed molecules as $\mathrm{d}\zeta_{ads} \propto \ln(N_{ox})$. In our case, ζ_{ads} is raised as the oxygen adsorption (corresponding to the cathodic reaction) proceeds, until ζ_{ads} becomes eventually equal to ζ_G (i.e., $\eta = 0$) and the net charge transfer occurs no more.

Type II-b: *The change in the work function of graphene by the electrical dipole layer formed between graphene and the adsorbed molecules with the finite charge.* This effect is owing to the field gradient (dipole layer) generated by the charge distribution between graphene and the adsorbed molecules. According to Poisson's equation, negative charge of the adsorbed oxygen molecules and the positive charge induced on graphene lowers the electrochemical potential of graphene in our case, which may change the relative level of ζ_{ads} with respect to ζ_{CNP}. The field gradient should depend on the adsorption structure, yet assuming that charge transfer between the adsorbed oxygen molecules and graphene occurs uniformly over the graphene surface, we can speculate that Type II-b effect is almost proportional to the adsorbed molecules.

Type II effects are related to the change in $\mathrm{d}(\zeta_{\mathrm{CNP}} - \zeta_{\mathrm{ads}})$ upon the increase of the adsorbed molecules. We envisage that Type II effects are represented as $\mathrm{d}(\zeta_{\mathrm{CNP}} - \zeta_{\mathrm{ads}}) \propto \mathrm{d}N_{\mathrm{ox}}$, as a matter of covenience.

Type III: *The inter-molecular interaction such as Coulomb repulsion between the adsorbed molecules.* This effect is an additional one corresponding to the term $\delta^{\ddagger}E$ in Eq. (S4); unlike the previous ones, the adsorption effect classified into Type III directly lifts up the energy barrier for charge transfer rather than changes the electrochemical potential of BLG. This would be prominent if the areal density of the adsorbed molecules is high. The change in ${}^{\ddagger}E$ by this effect is expected to be proportional to N_{ox} in the first approximation.

Since Type II and III effects are envisaged to have the same dependence on N_{ox} ($\approx \overline{n_{\mathrm{ox}}}/Z$), we can represent them shortly by

$$\mathrm{d}^{\ddagger}E_{\mathrm{II,III}} = \xi_{\mathrm{mol}}\mathrm{d}\overline{n_{\mathrm{ox}}} = -\xi_{\mathrm{mol}}D(\varepsilon_{\mathrm{F}})\mathrm{d}\varepsilon_{\mathrm{F}}, \tag{S5}$$

where we have used the relation $\mathrm{d}\overline{n_{\mathrm{ox}}} = -D(\varepsilon_{\mathrm{F}})\mathrm{d}\varepsilon_{\mathrm{F}}$. When the areal density of the adsorbed molecules is so low that Type II-b effect is dominant in Eq. (S5), ξ_{mol} is estimated within the plane capacitor model, in which the positive charges on graphene and the negative charges on the adsorbed molecules form charged layers apart from each other by the distance d . We have $\xi_{\mathrm{mol}} \sim \alpha ed/\varepsilon\varepsilon_0 \sim 10^{-18}$ eV m^2 where ε is the relative permittivity (as for the interface between graphene and the SiO_2 substrate, $\varepsilon = 2.5$) and ε_0 is the vacuum permittivity. When $\mathrm{d}\overline{n_{\mathrm{ox}}} \sim 10^{12}\mathrm{cm}^{-2}$ as in our case, the activation energy changes by $\mathrm{d}^{\ddagger}E_{\mathrm{II,III}} \sim 0.01$ eV. This is comparable with the shift of the Fermi level (i.e., Type I effect) and cannot be ignored.

Summing up all the molecular adsorption effects (ignoring Type IV effect), we acquire the relation equivalent to Eq. (2) in the main part:

$$\mathrm{d}^{\ddagger}E = -\alpha'\mathrm{d}\varepsilon_{\mathrm{F}} + \xi_{\mathrm{mol}}\mathrm{d}\overline{n_{\mathrm{ox}}} = -\alpha\mathrm{d}\varepsilon_{\mathrm{F}}, \tag{S6}$$

where we define the *pseudo* transfer coefficient α by

$$\alpha := \alpha' + \xi_{\mathrm{mol}}D(\varepsilon_{\mathrm{F}}) \tag{S7}$$

The activation energy ${}^{\ddagger}E$ is related to the overpotential η and the Fermi level ε_{F} by the transfer coefficient α' and the pseudo transfer coefficient α, respectively. Eq. (S7) shows us that α becomes greater than α' by $\xi_{\mathrm{mol}}\mathrm{d}\overline{n_{\mathrm{ox}}}$, to which we owe the anomalously large α_{te} (> 1) compared to the typical transfer coefficient for the electrochemical reaction: $\alpha' \sim 0.5$.

Importantly, the gate electric field changes ε_{F} as well as the molecular adsorption does, and thus changes the activation energy according to the discussion above. However, when only gate voltage is applied without molecular adsorption,[7] Type II and III effects are eliminated. Hence the second term of Eq. (S7) vanished and α is almost equal to α'. This is the reason that α_{gf}, which is calculated by the activation energy at $t = 0$ and does not affected by the molecular adsorption effect as mentioned above, is ca. 0.5.

Let us note the difference between our model based on the Butler–Volmer theory and that based on the Marcus–Gerischer model.[8–10] In our model, only the electron transfer at the energy of the transition state is considered, yet Marcus–Gerisher theory integrates the contribution of the charge transfer occurring at every energy level. Then the frequency of the charge transfer is given by

$$\frac{\mathrm{d}N_{\mathrm{ox}}}{\mathrm{d}t} = \chi W_0 \int_{-\infty}^{\infty} \mathrm{d}E \; f(E; \varepsilon_{\mathrm{F}} + \zeta_{\mathrm{CNP}}) D(E - \zeta_{\mathrm{CNP}}) \exp\left(-\frac{\{E - (E_{\mathrm{ads}} - \lambda)\}^2}{4k_{\mathrm{B}}T\lambda}\right), \tag{S8}$$

in Marcus–Gerischer theory where $f(E; \varepsilon_{\mathrm{F}} + \zeta_{\mathrm{CNP}}) = [(E - \varepsilon_{\mathrm{F}} - \zeta_{\mathrm{CNP}})/k_{\mathrm{B}}T + 1]^{-1}$ is the Fermi–Dirac distribution, $\lambda \sim 1$ eV is so-called reorganization energy, and $W_0 = \sqrt{4k_{\mathrm{B}}T\lambda}$ is the normalization factor. Note that Eq. (S8) is obtained by the substitution of $c_{\mathrm{ox}}\nu\kappa_{\mathrm{el}} = \chi D(E - \zeta_{\mathrm{CNP}})$ in Eq. (3) of Ref. 8, in which the effect by the factor of $D(E - \zeta_{\mathrm{CNP}})$ of the graphene electrode is ignored. Assuming $D(E - \zeta_{\mathrm{CNP}}) \sim D_{\mathrm{P}} = \gamma_{\perp}/\pi(\hbar v_{\mathrm{F}})$, we have $c_{\mathrm{ox}}\nu\kappa_{\mathrm{el}} \sim Z\chi\gamma_{\perp}/\pi(\hbar v_{\mathrm{F}})$, which is mentioned in the main part.

In contrast, our model (Eq. (3) in the main part) can be rewritten using Dirac δ function as

$$\frac{\mathrm{d}N_{\mathrm{ox}}}{\mathrm{d}t} = \chi \int_{-\infty}^{\infty} \mathrm{d}E \; f(E; \varepsilon_{\mathrm{F}} + \zeta_{\mathrm{CNP}}) D(E - \zeta_{\mathrm{CNP}}) \delta(E - \zeta_{\mathrm{TS}}), \tag{S9}$$

where $\zeta_{\mathrm{TS}} = {}^{\ddagger}E + \varepsilon_{\mathrm{F}} + \zeta_{\mathrm{CNP}}$ is determined by Eq. (2). The advantages of our model are that (i) the equation of the adsorption rate does not include the integral as in the Marcus–Gerisher model so that mathematical treatment is more feasible, and (ii) the various effects of molecular adsorption discussed above can be included via the pseudo transfer coefficient.

3 Temporal evolution of the charge doping

3.1 General expression for H kinetics model

The spectrum of the electric band of BLG is given by

$$\varepsilon_{\mathrm{F}}^{\pm\pm}(k) = \pm\sqrt{\varsigma_k^2 + \frac{\gamma_\perp^2}{2} \pm \sqrt{\frac{\gamma_\perp^4}{4} + \gamma_\perp^2\varsigma_k^2}}, \tag{S10}$$

where $\varsigma_k = \hbar v_{\mathrm{F}} k$ is the energy spectrum for SLG. Eq. (S10) is applicable near the CNP where the electronic band dispersion can be considered to be circularly symmetric. The first sign of the equation distinguishes the conduction bands and the valence bands, and the second sign does the higher energy bands and the lower energy bands. We can clearly figure out that the band dispersion of BLG is *hyperbolic* by transforming Eq. (S10) as

$$\left(\varepsilon_{\mathrm{F}}(k) \pm \frac{\gamma_\perp}{2}\right)^2 - (\hbar v_{\mathrm{F}} k)^2 = \frac{\gamma_\perp^2}{4}, \tag{S11}$$

where for $\varepsilon_{\mathrm{F}}(k) \geq 0$ the band with the positive (negative) sign corresponds to the lower (higher) energy band, and for $\varepsilon_{\mathrm{F}}(k) \leq 0$ the band with the positive (negative) sign corresponds to the higher (lower) energy band. In the vicinity of the CNP where $|\varepsilon_{\mathrm{F}}| \ll \gamma_\perp/2 \approx 0.2$ eV is applicable, Eq. (S11) approximately turns parabolic,

$$\varepsilon_{\mathrm{F}}(k) = \pm\frac{(\hbar v_{\mathrm{F}} k)^2}{\gamma_\perp} \tag{S12}$$

The DOS of BLG is given by[11]

$$D(\varepsilon_{\mathrm{F}}) = \begin{cases} \dfrac{1}{\pi(\hbar v_{\mathrm{F}})^2}(2|\varepsilon_{\mathrm{F}}| + \gamma_\perp), & \text{for } |\varepsilon_{\mathrm{F}}| < \gamma_\perp \quad \text{(S13a)} \\ \dfrac{4}{\pi(\hbar v_{\mathrm{F}})^2}|\varepsilon_{\mathrm{F}}|, & \text{for } |\varepsilon_{\mathrm{F}}| \geq \gamma_\perp \quad \text{(S13b)} \end{cases}$$

Note that there is a jump of the DOS at the bottom of the high energy band, i.e., $|\varepsilon_{\mathrm{F}}| = \gamma_\perp$.

Let us write the integration form of Eq. (4):

$$-\frac{\alpha_{\mathrm{te}}}{k_{\mathrm{B}}T}\exp\left(\alpha_{\mathrm{te}}\frac{\varepsilon_{\mathrm{F},0}}{k_{\mathrm{B}}T}\right)\int_I \mathrm{d}\varepsilon'_{\mathrm{F}}\,\exp\left(-\alpha_{\mathrm{te}}\frac{\varepsilon'_{\mathrm{F}}}{k_{\mathrm{B}}T}\right)\frac{D(\varepsilon'_{\mathrm{F}})}{D\left(\varepsilon'_{\mathrm{F}} + {}^{\ddagger}E(\varepsilon'_{\mathrm{F}})\right)} = pt, \tag{S14}$$

where $I = [\varepsilon_{\mathrm{F},0}, \varepsilon_{\mathrm{F}}]$ is the interval of integration. Herein we assume that $\alpha_{\mathrm{te}} \neq 0, 1$. When the parabolic approximation is available, the DOS can be envisaged as constant: $D(\varepsilon_{\mathrm{F}}) = D_{\mathrm{P}} = \gamma_{\perp}/\pi(\hbar v_{\mathrm{F}})^2$. Then we can obtain the expression P kinetics, given by Eq. (6).

For the derivation of H kinetics, we assign $D(\varepsilon_{\mathrm{F}}) = (2|\varepsilon_{\mathrm{F}}| + \gamma_{\perp})/\pi(\hbar v_{\mathrm{F}})^2$ to the DOS at the Fermi level, since the Fermi level fulfills $|\varepsilon_{\mathrm{F}}| < \gamma_{\perp} = 0.4$ eV in the present study (see Figure 6(c)). On the other hand for the DOS at the level of the transition state, it is reasonable to use $D\left(\varepsilon_{\mathrm{F}} + {}^{\ddagger}E(\varepsilon_{\mathrm{F}})\right) = 4|\varepsilon_{\mathrm{F}} + {}^{\ddagger}E(\varepsilon_{\mathrm{F}})|/\pi(\hbar v_{\mathrm{F}})^2$, the DOS in which the higher energy band is included, since we find that $\varepsilon_{\mathrm{F}} + {}^{\ddagger}E(\varepsilon_{\mathrm{F}})$ is higher than $\gamma_{\perp}$ except in the short O_2-exposure-time regime for $V_{\mathrm{g,ad}} = -50$ V (for which $\varepsilon_{\mathrm{F}} + {}^{\ddagger}E(\varepsilon_{\mathrm{F}})$ is slightly lower than 0.4 eV). From Eq. (2) in the main part, we have

$$\varepsilon_{\mathrm{F}} + {}^{\ddagger}E(\varepsilon_{\mathrm{F}}) = \varepsilon_{\mathrm{F}} + \left[{}^{\ddagger}E(\varepsilon_{\mathrm{F},0}) - \alpha_{\mathrm{te}}(\varepsilon_{\mathrm{F}} - \varepsilon_{\mathrm{F},0})\right] \tag{S15}$$

Hence we obtain

$$\begin{aligned} D\left(\varepsilon_{\mathrm{F}} + {}^{\ddagger}E(\varepsilon_{\mathrm{F}})\right) &= \frac{4\left[\varepsilon_{\mathrm{F}} + {}^{\ddagger}E(t)\right]}{\pi(\hbar v_{\mathrm{F}})^2} \\ &= \frac{4}{\pi(\hbar v_{\mathrm{F}})^2}\left[(1-\alpha_{\mathrm{te}})\varepsilon_{\mathrm{F}} + \alpha_{\mathrm{te}}\varepsilon_{\mathrm{F},0} + {}^{\ddagger}E(\varepsilon_{\mathrm{F},0})\right] \end{aligned} \tag{S16}$$

Defining $b = \left[\alpha_{\mathrm{te}}\varepsilon_{\mathrm{F},0} + {}^{\ddagger}E(\varepsilon_{\mathrm{F},0})\right]/(1-\alpha_{\mathrm{te}})$, we can transform the integration term in Eq. (S14) as follows:

$$\begin{aligned} S[\varepsilon_{\mathrm{F},0}, \varepsilon_{\mathrm{F}}] &= \int_I \mathrm{d}\varepsilon'_{\mathrm{F}}\ \exp\left(-\alpha_{\mathrm{te}}\frac{\varepsilon'_{\mathrm{F}}}{k_{\mathrm{B}}T}\right)\frac{D(\varepsilon'_{\mathrm{F}})}{D(\varepsilon'_{\mathrm{F}} + {}^{\ddagger}E(\varepsilon'_{\mathrm{F}}))} \\ &= \int_I \mathrm{d}\varepsilon'_{\mathrm{F}}\ \exp\left(-\alpha_{\mathrm{te}}\frac{\varepsilon'_{\mathrm{F}}}{k_{\mathrm{B}}T}\right)\frac{2|\varepsilon'_{\mathrm{F}}| + \gamma_{\perp}}{4(1-\alpha_{\mathrm{te}})(\varepsilon'_{\mathrm{F}} + b)} \\ &= \frac{1}{2(1-\alpha_{\mathrm{te}})}\int_I \mathrm{d}\varepsilon'_{\mathrm{F}}\ \mathrm{sgn}(\varepsilon'_{\mathrm{F}})\exp\left(-\alpha_{\mathrm{te}}\frac{\varepsilon'_{\mathrm{F}}}{k_{\mathrm{B}}T}\right)\left(1 + \frac{\mathrm{sgn}(\varepsilon'_{\mathrm{F}})\gamma_{\perp}/2 - b}{\varepsilon'_{\mathrm{F}} + b}\right) \\ &= \frac{1}{2(1-\alpha_{\mathrm{te}})}\left[\mp\frac{k_{\mathrm{B}}T}{\alpha_{\mathrm{te}}}e^{-\frac{\alpha_{\mathrm{te}}}{k_{\mathrm{B}}T}\varepsilon'_{\mathrm{F}}} + \left(\frac{\gamma_{\perp}}{2} \mp b\right)e^{\frac{\alpha_{\mathrm{te}}}{k_{\mathrm{B}}T}b}\,\mathrm{Ei}\left(-\frac{\alpha_{\mathrm{te}}}{k_{\mathrm{B}}T}(\varepsilon'_{\mathrm{F}} + b)\right)\right]_I \end{aligned} \tag{S17}$$

where $\mathrm{sgn}(x)$ is the sign function, $\mathrm{Ei}(x)$ is the exponential integral defined by $\mathrm{Ei}(x) = -\int_{-x}^{\infty} e^{-t}/t\ \mathrm{d}t$, and $[F(\varepsilon'_{\mathrm{F}})]_I := F(\varepsilon_{\mathrm{F}}) - F(\varepsilon_{\mathrm{F},0})$ for an arbitrary function $F(\varepsilon'_{\mathrm{F}})$. The double signs are in same order, and the upper (lower) signs are taken when the interval I is in the higher (lower) regime than the level of the CNP. If the interval I includes the CNP (i.e., $\varepsilon_{\mathrm{F},0} > 0$ while

Table.S1 Difference in the pseudo transfer coefficient and the activation energy for various gate voltage $V_{g,ad}$ by the density of states of BLG at the level of the transition state: with/without including the higher energy band (HE band), or the constant density of states

	Pseudo transfer coefficient α_{te}			Initial activation energy ${}^{\ddagger}E\,(\varepsilon_{F,0})$ (eV)		
$V_{g,ad}$	with HE band $\frac{4\lvert\varepsilon_F+{}^{\ddagger}E(\varepsilon_F)\rvert}{\pi(\hbar v_F)^2}$	without HE band $\frac{2\lvert\varepsilon_F+{}^{\ddagger}E(\varepsilon_F)\rvert+\gamma_\perp}{\pi(\hbar v_F)^2}$	constant $\frac{4\lvert\varepsilon_{F,0}+{}^{\ddagger}E(\varepsilon_{F,0})\rvert}{\pi(\hbar v_F)^2}$	with HE band $\frac{4\lvert\varepsilon_F+{}^{\ddagger}E(\varepsilon_F)\rvert}{\pi(\hbar v_F)^2}$	without HE band $\frac{2\lvert\varepsilon_F+{}^{\ddagger}E(\varepsilon_F)\rvert+\gamma_\perp}{\pi(\hbar v_F)^2}$	constant $\frac{4\lvert\varepsilon_{F,0}+{}^{\ddagger}E(\varepsilon_{F,0})\rvert}{\pi(\hbar v_F)^2}$
+80	1.56	1.55	1.54	0.40	0.39	0.40
+40	1.39	1.38	1.37	0.44	0.43	0.44
0	2.04	2.02	1.98	0.46	0.46	0.46
−50	3.18	3.14	3.05	0.50	0.49	0.50

$\varepsilon_F < 0$), the integration is performed in each regime:

$$S[\varepsilon_{F,0},\varepsilon_F] = \frac{1}{2(1-\alpha_{te})}\left[\int_0^{\varepsilon_F} d\varepsilon'_F\ \exp\left(-\alpha_{te}\frac{\varepsilon'_F}{k_BT}\right)\frac{\varepsilon'_F+\gamma_\perp/2}{\varepsilon'_F+b} + \int_{\varepsilon_{F,0}}^{0} d\varepsilon'_F\ \exp\left(-\alpha_{te}\frac{\varepsilon'_F}{k_BT}\right)\frac{-\varepsilon'_F+\gamma_\perp/2}{\varepsilon'_F+b}\right] \quad \text{(S18)}$$

Then we obtain the H kinetics expression of the temporal evolution of doping in an integrated form,

$$pt = -\frac{\alpha_{te}}{k_BT}\exp\left(\alpha_{te}\frac{\varepsilon_{F,0}}{k_BT}\right)S[\varepsilon_{F,0},\varepsilon_F], \quad \text{(S19)}$$

where the integration $S[\varepsilon_F,\varepsilon_{F,0}]$ is given by Eqs. (S17) and (S18) . Note that the expression for $D(\varepsilon_F+{}^{\ddagger}E(\varepsilon_F))$ is not significant; we have taken the higher energy band $D(\varepsilon_F)=4|\varepsilon_F(t)|/\pi(\hbar v_F)^2$ in the derivation above, yet the results hardly change if we use the lower energy band $D(\varepsilon_F)=(2|\varepsilon_F|+\gamma_\perp)/\pi(\hbar v_F)^2$. Even if we assume the DOS of the transition state level is constant: $D(\varepsilon_F+{}^{\ddagger}E(\varepsilon_F)) = D(\varepsilon_{F,0}+{}^{\ddagger}E(\varepsilon_{F,0}))$ (temporally invariant) , i.e.,

$$S[\varepsilon_{F,0},\varepsilon_F] = \frac{1}{2(\varepsilon_{F,0}+{}^{\ddagger}E(\varepsilon_{F,0}))}\left[\left(-\frac{k_BT}{\alpha_{te}}\right)\left\{\left(\pm\varepsilon'_F+\frac{\gamma_\perp}{2}\right)\pm\left(\frac{k_BT}{\alpha_{te}}\right)\right\}\exp\left(-\alpha_{te}\frac{\varepsilon'_F}{k_BT}\right)\right]_I, \quad \text{(S20)}$$

where the upper (lower) sign is taken when I in the higher (lower) regime than the level of the CNP, and $S[\varepsilon_{F,0},\varepsilon_F]$ is obtained by $S[\varepsilon_{F,0},0]+S[0,\varepsilon_F]$ when I includes the CNP, as in Eq. (S18). The results for various way of assignment of $D(\varepsilon_F+{}^{\ddagger}E(\varepsilon_F))$ are summarized in Table S1.

If the Fermi level is away from the CNP by more than $\gamma_\perp$, the electrons in the higher energy band also contribute to charge transfer, which would result in the increase of the rate for doping. Reported values of $\gamma_\perp$ vary within 0.2–0.4 eV.[12,13] On the other hand, in our study, the largest $|\varepsilon_\mathrm{F}|$ is realized when the sum of the carriers induced by the gate electric field and the adsorbed oxygen is the largest, i.e., the device applied with $V_{\mathrm{g,ad}} = -50$ V and exposed to oxygen for the longest time. Even for such case the Fermi energy is, however, in the region of $|\varepsilon_\mathrm{F}| \lesssim 0.19$ eV for $\gamma_\perp = 0.4$ eV as shown in Figure 6(c) (H kinetics) in the main part. Therefore we need not take the contribution of the higher energy band into consideration (note that if $\gamma_\perp = 0.22$ eV is applied, the range of the Fermi level extends up to $|\varepsilon_\mathrm{F}| \lesssim 0.24$ eV and the contribution of the higher energy band should be included). It is reported[14] that highly doped BLG accomplished by electric double layer shows non-monotonic behavior in σ vs V_g, which is attributed to the effect of inter-band scattering between the higher energy band and lower energy band. Yet we cannot find such behavior in σ vs V_g curve of $V_{\mathrm{g,ad}} = -50$ V, which supports no contribution of the high energy band to the kinetics of adsorption.

3.2 Gap-opening effect due to asymmetric adsorption

One of the interesting features for BLG is band-gap opening caused by an asymmetrical biasing between the top and bottom layers. First we derive the DOS of the gapped BLG.[13,15] By parameterizing the potential asymmetry between layers by the energy difference V, the energy spectrum of the biased BLG is given by the well-known Mexican-hat like dispersion:

$$\varepsilon_\mathrm{F}^{\pm\pm}(k,V) = \pm\sqrt{\varsigma_k^2 + \frac{\gamma_\perp^2}{2} + \frac{V^2}{4} \pm \sqrt{\frac{\gamma_\perp^4}{4} + (t_\perp^2 + V^2)\varsigma_k^2}}, \tag{S21}$$

where $\varsigma_k = \hbar v_\mathrm{F} k$. Transforming Eq. (S21), we have an equation with respect to ς_k^2:

$$F\left(\varsigma_k^2\right) = \left(\varsigma_k^2\right)^2 - \left(\frac{V^2}{2} + 2\varepsilon_\mathrm{F}^2\right)\varsigma_k^2 + \left\{\varepsilon_\mathrm{F}^4 - \left(\gamma_\perp^2 + \frac{V^2}{2}\right)\varepsilon_\mathrm{F}^2 + \frac{V^4}{16} + \frac{\gamma_\perp^2 V^2}{4}\right\} = 0 \tag{S22}$$

By considering the condition for Eq. (S22) to have the positive solution, we can classify the energy region as follows:

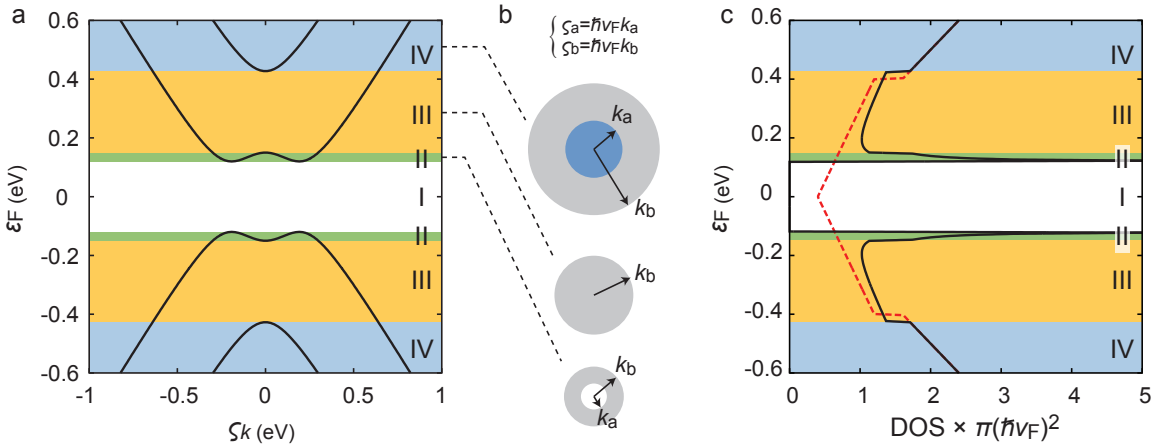

Figure.S1 (a) Spectrum of the gapped BLG plotted with respect to ς_k ($= \hbar v_F k$), calculated in the case of $V = 0.3$ eV and $\gamma_\perp = 0.4$ eV. (b) Cross section of the k-space orbit at the energy ε_F for Region II–IV. The arrows denotes the radius. The blue region for Region IV represents the Fermi surface of the high energy band. (c) DOS of the gapped BLG (black solid line) and of the gapless BLG (red dashed line).

Region (I): *in the band gap* for

$$|\varepsilon_F| < \frac{\gamma_\perp |V|}{2\sqrt{\gamma_\perp^2 + V^2}},$$

where Eq. (S22) has no solutions. The gap width is given by $\gamma_\perp |V| / \sqrt{\gamma_\perp^2 + V^2}$.

Region (II): *between the bottom and the top of the Mexican hat* for

$$\frac{\gamma_\perp |V|}{2\sqrt{\gamma_\perp^2 + V^2}} \le |\varepsilon_F| \le \frac{|V|}{2},$$

where Eq. (S22) has two positive solution $\varsigma_k^2 = \varsigma_a^2, \varsigma_b^2$ ($0 \le \varsigma_a^2 \le \varsigma_b^2$, including double roots). Cross-section area enclosed by the orbit of energy ε_F in k- space ($= \pi^2 n(\varepsilon_F)$) is given by

$$A_k^{\mathrm{II}} = \frac{\pi}{(\hbar v_F)^2}(\varsigma_b^2 - \varsigma_a^2) = \frac{\pi}{(\hbar v_F)^2}\sqrt{4(\gamma_\perp^2 + V^2)\varepsilon_F^2 - \gamma_\perp^2 V^2} \qquad \text{(S23a)}$$

Region (III): *between the top of the Mexican hat and the bottom of the high energy band* for

$$\frac{|V|}{2} < |\varepsilon_{\mathrm{F}}| < \frac{\sqrt{4\gamma_\perp^2 + V^2}}{2}$$

where Eq. (S22) has one positive solution $\varsigma_k^2 = \varsigma_{\mathrm{b}}^2$. We have

$$A_k^{\mathrm{III}} = \frac{\pi}{(\hbar v_{\mathrm{F}})^2}\varsigma_{\mathrm{b}}^2 = \frac{\pi}{(\hbar v_{\mathrm{F}})^2} \times \frac{1}{2}\left[\frac{V^2}{2} + 2\varepsilon_{\mathrm{F}}^2 + \sqrt{4(\gamma_\perp^2 + V^2)\varepsilon_{\mathrm{F}}^2 - \gamma_\perp^2 V^2}\right] \quad \text{(S23b)}$$

Region (IV): *in the region where the high energy band participates* for

$$\sqrt{\gamma_\perp^2 + \frac{V^2}{4}} \leq |\varepsilon_{\mathrm{F}}|$$

where Eq. (S22) has two positive solution $\varsigma_k^2 = \varsigma_{\mathrm{a}}^2, \varsigma_{\mathrm{b}}^2$ ($0 \leq \varsigma_{\mathrm{a}}^2 < \varsigma_{\mathrm{b}}^2$, including double roots). Note that in this region we give the area A_k^{IV} by the sum of those of the high energy band and the low energy band:

$$A_k^{\mathrm{IV}} = \frac{\pi}{(\hbar v_{\mathrm{F}})^2}\varsigma_{\mathrm{b}}^2 + \frac{\pi}{(\hbar v_{\mathrm{F}})^2}\varsigma_{\mathrm{a}}^2 = \frac{\pi}{(\hbar v_{\mathrm{F}})^2}\left(\frac{V^2}{2} + 2\varepsilon_{\mathrm{F}}^2\right) \quad \text{(S23c)}$$

In each region we acquire the DOS by calculating $D(\varepsilon_{\mathrm{F}}) = (1/\pi^2)\,|\mathrm{d}A/\mathrm{d}\varepsilon_{\mathrm{F}}|$ as

$$\begin{cases} D^{\mathrm{I}}(\varepsilon_{\mathrm{F}}) = 0 & \text{(S24a)} \\ D^{\mathrm{II}}(\varepsilon_{\mathrm{F}}) = \dfrac{4|\varepsilon_{\mathrm{F}}|}{\pi(\hbar v_{\mathrm{F}})^2} \dfrac{\gamma_\perp^2 + V^2}{\sqrt{4(\gamma_\perp^2 + V^2)\varepsilon_{\mathrm{F}}^2 - \gamma_\perp^2 V^2}} & \text{(S24b)} \\ D^{\mathrm{III}}(\varepsilon_{\mathrm{F}}) = \dfrac{2|\varepsilon_{\mathrm{F}}|}{\pi(\hbar v_{\mathrm{F}})^2}\left[1 + \dfrac{\gamma_\perp^2 + V^2}{\sqrt{4(\gamma_\perp^2 + V^2)\varepsilon_{\mathrm{F}}^2 - \gamma_\perp^2 V^2}}\right] & \text{(S24c)} \\ D^{\mathrm{IV}}(\varepsilon_{\mathrm{F}}) = \dfrac{4|\varepsilon_{\mathrm{F}}|}{\pi(\hbar v_{\mathrm{F}})^2} & \text{(S24d)} \end{cases}$$

Singularities are found on the boundary between the regions.

Next we roughly estimate V for the case of our experiments, in the way as is shown in the literature.[11,13] Let us consider that BLG feels the molecular field by the adsorbed molecules with

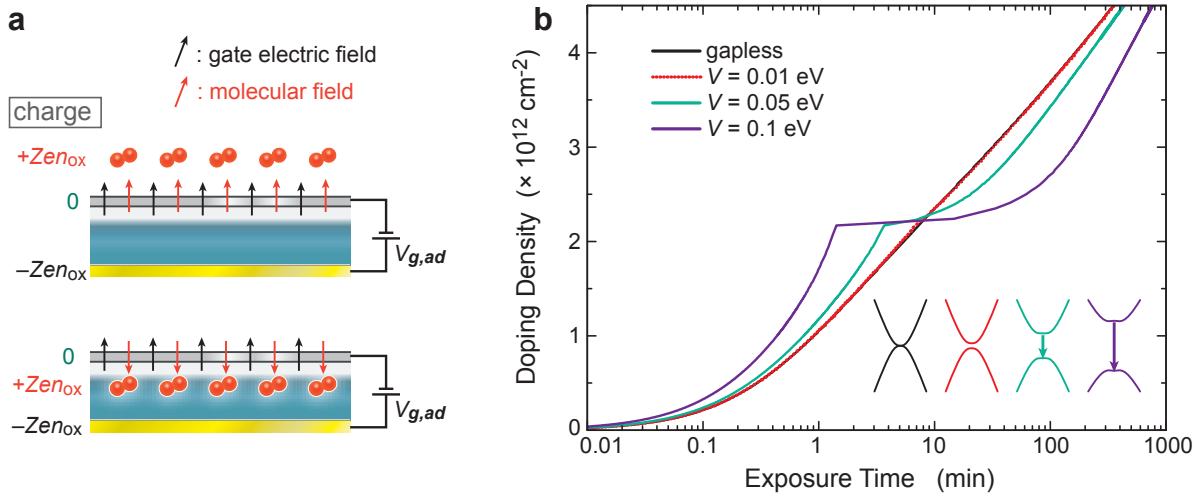

Figure.S2 Electric field gradient due to molecular adsorption and its effect on the time evolution of adsorption via gap opening. (a) Combination of electric field of the gate electric field (black arrow) and the molecular field (red arrow) generated by the negative charge on adsorbed molecules. At the CNP, where charge density of BLG is adjusted to 0 by a positive gate voltage, the electric field enhances (destructs) each other when molecules adsorb on the top of graphene (in the interface). (b) Theoretical calculation of the time evolution of the doping, for the gapped BLG due to the electric field gradient between top and bottom layers. The abrupt change of the curve occurs when the Fermi level moves across the band gap (inset).

net charge $Ze\overline{n_{ox}}$ ($Z < 0$ in our case of the oxygen adsorption) as well as the gate electric field. The net electric field differs by whether the molecules adsorb on the top of BLG (top panel of Figure S2(a)) or in the interface between BLG and the SiO_2 substrate (the bottom panel of Figure S2(a)). In the former case, the gate electric field and the molecular field reinforce each other and the energy difference between layers is enhanced, when $V_{g,ad}$ has the opposite sign against Z. On the other hand in the latter case, V becomes large when Z and $V_{g,ad}$ have the same sign. The chemisorption of oxygen in our electrochemical model corresponds to the latter case (Figure 4(a), inset), and therefore the band gap becomes the largest on the condition that highly negative $V_{g,ad}$ is applied and a large amount of oxygen is adsorbed. However, the Fermi level is far away from the CNP at that time. To tune the Fermi level to around the CNP, we have to apply a positive $V_{g,ad}$ until the doping density by the adsorbed molecules and that by the electric field are balanced so that the induced charge on graphene is adjusted to zero. Instead, V becomes the smallest since

the gate electric field and the molecular field destruct each other. Hence we should not catch the effect of opening band gap to the adsorption kinetics.

If we consider that the molecules adsorb on the top side of graphene opposite to the gate electrode, a finite gap exists when the Fermi level crosses the CNP. Taking the direction from the gate electrode to BLG as the positive direction, the gate electric field is given by $E_{\mathrm{g}} = c_{\mathrm{g}} V_{\mathrm{g,ad}}/\varepsilon\varepsilon_0$ and the molecular field is approximately given by $E_m = -Ze\overline{n_{\mathrm{ox}}}/\varepsilon\varepsilon_0$, if molecules adsorb homogeneously at the distance of d from graphene. Ignoring the screening effect, $V = ed_{\mathrm{C-C}}(E_{\mathrm{g}} + E_{\mathrm{m}})$ is obtained with the distance between layers of BLG $d_{\mathrm{C-C}} = 0.335$ nm.[16,17] Hence $V = 2ed_{\mathrm{C-C}} c_{\mathrm{g}} V_{\mathrm{g,ad}}/\varepsilon\varepsilon_0$ is obtained when the Fermi level is tuned to the CNP (i.e., $c_{\mathrm{g}} V_{\mathrm{g}} = -Ze\overline{n_{\mathrm{ox}}}$). According to this model, the gap width $\gamma_\perp |V|/(\gamma_\perp^2 + V^2)^{1/2}$ is 0.116 eV ($V = 0.122$ eV) at the CNP when $V_{\mathrm{g,ad}} = 40$ V is applied. This is large enough to affect the kinetics.

In Figure 2 in the main part, we can find that the experimental results exhibit a small wobbles against the theoretical curve acquired by fitting under the *gapless* condition around the CNP (pointed by the arrow 5) for $V_{\mathrm{g,ad}} = +40$ V. This can be related to the gap-opening effect. By numerical calculation using Eqs. (S14) and (S24a)–(S24d), we simulate the evolution of hole doping with the O_2 exposure time, for various potential differences V (Figure S2(b)). For ease in comparison with the experimental results (Figure 2), we use the parameters α_{te} and p acquired by fitting to the results of $V_{\mathrm{g,ad}} = +40$ V under gapless H kinetics model, taking the total doping density in common irrespective of V. For $V = 0.01$ eV, the band gap (the gap width is almost equal to $|V|$ when $|V| \ll \gamma_\perp$) gives only a small effect to $\overline{n_{\mathrm{ox}}}$ vs t curve. Yet for larger V, a significant deviation from the gapless results is invoked; while the Fermi level is beyond the bottom of conduction band, the hole doping (or the molecular adsorption) proceeds more rapidly for the gapped BLG than the gapless BLG. Then the rate for adsorption suddenly decreases at the doping density of $\overline{n_{\mathrm{ox}}} = 2.2 \times 10^{12}$ cm^{-2}, and after that the rate is even suppressed compared with the gapless BLG. These behaviors are because of the singularity in DOS near the edges of the band gap (Figure S1(c)). When the Fermi level is in the conduction band, the DOS at the Fermi energy for gapped BLG is larger than that of gapless BLG. Thus the downward shift of the Fermi level accompanied with the oxygen adsorption is suppressed, resulting in enhancing the electron transfer, especially at the proximity of the bottom of the conduction band. When all the electrons are drained from the conduction band, the charge transfer has to be brought about by the electrons in the valence band; then an abrupt increase as large as $\sim \alpha_{\mathrm{te}} V$ occurs in the activation energy for

the charge transfer. Once the Fermi level moves into the valence band, the DOS of the gapped BLG is larger than that of the gapless BLG similarly to the conduction band. Hence the difference of the doping density between the gapped and the gapless BLG decreases with time. Note that in the actual adsorption, V should vary with increasing amount of the adsorption because of the temporal change of the molecular field. Therefore the time evolution of the doping is likely to deviate from the estimation shown in Figure S2(b), though the behavior around the CNP will not change substantially.

References for Supporting Information

(1) Malard, L. M.; Pimenta, M. A.; Dresselhaus, G.; Dresselhaus, M. *Phys. Rep.* **2009**, *473*, 51–87.

(2) Ni, Z.; Wang, Y.; Yu, T.; You, Y.; Shen, Z. *Phys. Rev. B* **2008**, *77*, 235403.

(3) Poncharal, P.; Ayari, A.; Michel, T.; Sauvajol, J. L. *Phys. Rev. B* **2008**, *78*, 113407.

(4) Sagar, A.; Lee, E. J. H.; Balasubramanian, K.; Burghard, M.; Kern, K. *Nano Lett.* **2009**, *9*, 3124–3128.

(5) Teweldebrhan, D.; Balandin, A. A. *Appl. Phys. Lett.* **2009**, *94*, 013101.

(6) Bockris, J. O. M.; Nagy, Z. *J. Chem. Educ.* **1973**, *50*, 839.

(7) Yu, Y.-J.; Zhao, Y.; Ryu, S.; Brus, L. E.; Kim, K. S.; Kim, P. *Nano Lett.* **2009**, *9*, 3430–3434.

(8) Levesque, P. L.; Sabri, S. S.; Aguirre, C. M.; Guillemette, J.; Siaj, M.; Desjardins, P.; Szkopek, T.; Martel, R. *Nano Lett.* **2010**, *11*, 132–137.

(9) Sharma, R.; Nair, N.; Strano, M. S. *J. Phys. Chem. C* **2009**, *113*, 14771–14777.

(10) Heller, I.; Kong, J.; Williams, K. A.; Dekker, C.; Lemay, S. G. *J. Am. Chem. Soc.* **2006**, *128*, 7353–7359.

(11) Castro, E. V.; Novoselov, K. S.; Morozov, S. V.; Peres, N. M. R.; dos Santos, J. M. B. L.; Nilsson, J.; Guinea, F.; Geim, A. K.; Castro Neto, A. H. *Phys. Rev. Lett.* **2007**, *99*, 216802.

(12) Castro Neto, A. H.; Guinea, F.; Peres, N. M. R.; Novoselov, K. S.; Geim, A. K. *Rev. Mod. Phys.* **2009**, *81*, 109–162.

(13) Castro, E. V.; Novoselov, K. S.; Morozov, S. V.; Peres, N. M. R.; Lopes dos Santos, J. M. B.; Nilsson, J.; Guinea, F.; Geim, A. K.; Castro Neto, A. H. *J. Phys.: Condens. Matter* **2010**, *22*, 175503.

(14) Ye, J.; Craciun, M. F.; Koshino, M.; Russo, S.; Inoue, S.; Yuan, H.; Shimotani, H.; Morpurgo, A. F.; Iwasa, Y. *Proc. Natl. Acad. Sci. U.S.A.* **2011**, doi:10.1073/pnas.1018388108.

(15) Castro, E. V.; Peres, N. M. R.; Lopes dos Santos, J. M. B. *Phys. Status Solidi B* **2007**, *244*, 2311–2316.

(16) Franklin, R. E. *Acta Cryst.* **1951**, *4*, 253–261.

(17) Enoki, T.; Endo, M.; Suzuki, M. *Graphite intercalation compounds and applications*; Oxford University Press: New York, 2003.